

1 **Supplementary Table 1**

2 **Gene clone ID for ShRNA-mediated gene silencing TNF α downstream signals in *in vitro***

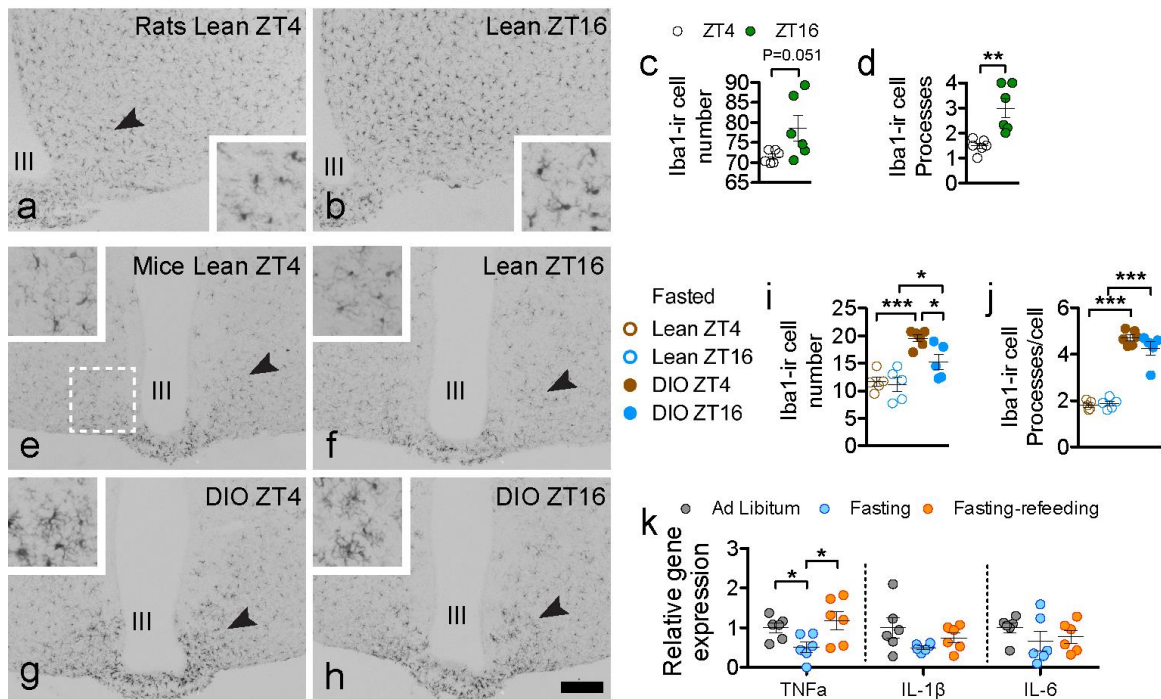
3

4 Symbol	Gene ID	RefSeqID	Clone ID
6 ATP6v1e2	74915	NM_029121	TRCN0000103700
7			TRCN0000103701
8			TRCN0000103702
9			TRCN0000103703
10			TRCN0000103704
11 BIRC2	11797	NM_007465	TRCN0000012303
12			TRCN0000012304
13			TRCN0000012305
14			TRCN0000012306
15			TRCN0000012307
16 CD40	21939	NM_011611	TRCN0000066243
17			TRCN0000066244
18			TRCN0000066245
19			TRCN0000066246
20 Cox6a2	12862	NM_009943	TRCN0000076809
21			TRCN0000076810
22			TRCN0000076811
23			TRCN0000076812
24 IKK β	16150	NM_010546	TRCN0000026867
25			TRCN0000026891
26			TRCN0000026894
27			TRCN0000026913
28			TRCN0000026945
29 Map2k6 (MKK6)	26399	NM_011943	TRCN0000025259
30			TRCN0000025260
31			TRCN0000025261
32			TRCN0000025262
33			TRCN0000025263
34 Ndufab1	70316	NM_028177	TRCN0000041878
35			TRCN0000041879
36			TRCN0000041880
37			TRCN0000041881
38			TRCN0000041882
39 NF κ B1	18033	NM_008689	TRCN0000009510
40			TRCN0000009511
41			TRCN0000009512
42			TRCN0000009513
43			TRCN0000009514
44 Park2 (Parkin)	50873	NM_016694	TRCN0000041143

45				TRCN0000041144
46				TRCN0000041145
47				TRCN0000041146
48				TRCN0000041447
49	PINK1	68943	NM_026880	TRCN0000026727
50				TRCN0000026733
51				TRCN0000026742
52				TRCN0000026743
53				TRCN0000026750
54	Stat3	20848	NM_011486	TRCN0000071453
55				TRCN0000071454
56				TRCN0000071455
57				TRCN0000071456
58				TRCN0000071457
59	Nr2c2 (TAK1)	22026	XM_132700	TRCN0000027044
60				TRCN0000027072
61				TRCN0000027073
62				TRCN0000027089
63	TNFRsf1a	21937	NM_011609	TRCN0000066103
64				TRCN0000066104
65				TRCN0000066105
66				TRCN0000066106
67				TRCN0000066107
68	TNFRsf1b	21938	NM_011610	TRCN0000012318
69				TRCN0000012319
70				TRCN0000012320
71				TRCN0000012321
72				TRCN0000012322
73	TNFRsf4	22163	NM_011659	TRCN0000066193
74				TRCN0000066194
75				TRCN0000066195
76				TRCN0000066196
77				TRCN0000066197
78	Tnfrsf6	18053	NM_033217	TRCN0000065553
79				TRCN0000065554
80				TRCN0000065555
81				TRCN0000065556
82				TRCN0000065557
83	TNFRsf10b	21933	NM_020275	TRCN0000012323
84				TRCN0000012324
85				TRCN0000012325
86				TRCN0000012326
87				TRCN0000012327
88	TNFRsf11a	21934	NM_009399	TRCN0000065698

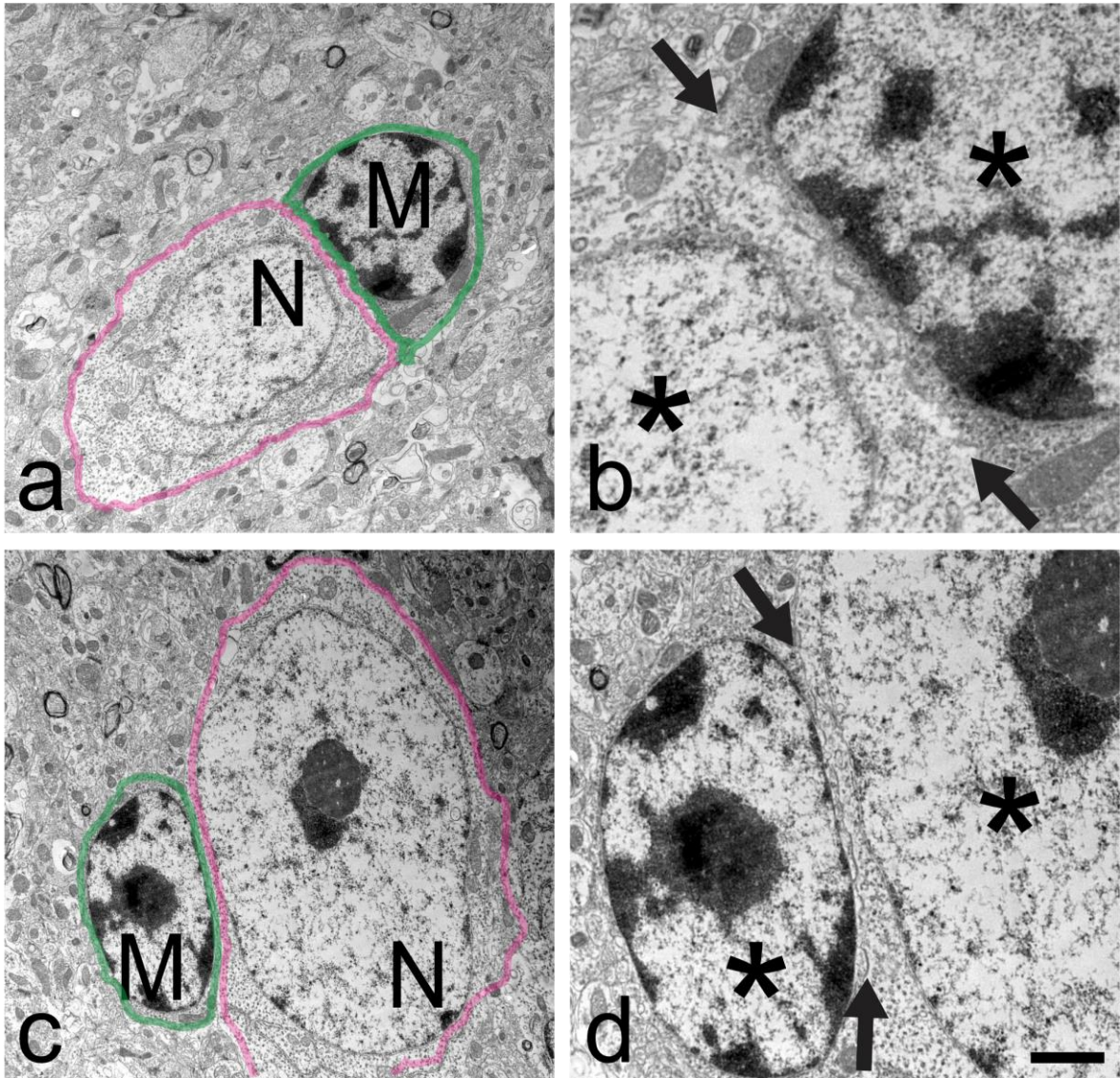
89				TRCN0000065699
90				TRCN0000065700
91				TRCN0000065701
92				TRCN0000065702
93	TNFrsf11b	18383	NM_008764	TRCN0000065748
94				TRCN0000065749
95				TRCN0000065750
96				TRCN0000065751
97				TRCN0000065752
98	TNFrsf12a	27279	NM_013749	TRCN0000066883
99				TRCN0000066884
100				TRCN0000066885
101				TRCN0000066886
102				TRCN0000066887
103	TNFrsf13c	72049	NM_028075	TRCN0000066733
104				TRCN0000066734
105				TRCN0000066735
106				TRCN0000066736
107				TRCN0000066737
108	TNFrsf14	230979	NM_178931	TRCN0000065853
109				TRCN0000065854
110				TRCN0000065855
111				TRCN0000065856
112				TRCN0000065857
113	Tnfrsf16	14102	NM_007987	TRCN0000012328
114				TRCN0000012329
115				TRCN0000012330
116				TRCN0000012331
117				TRCN0000012332
118	TNFrsf17	21935	NM_011608	TRCN0000065898
119				TRCN0000065899
120				TRCN0000065900
121				TRCN0000065901
122				TRCN0000065902
123	TNFrsf18	21936	NM_009400	TRCN0000065953
124				TRCN0000065954
125				TRCN0000065955
126				TRCN0000065956
127				TRCN0000065957
128	TNFrsf21	94185	NM_052975	TRCN0000066598
129				TRCN0000066599
130				TRCN0000066600
131				TRCN0000066601
132				TRCN0000066602

133	TRADD	71609	NM_001033161	TRCN0000178874
134				TRCN0000179091
135				TRCN0000183578
136				TRCN0000184240
137	TRAF2	22030	NM_009422	TRCN0000077228
138				TRCN0000077229
139				TRCN0000077230
140				TRCN0000077231
141				TRCN0000077232
142	TRAF5	22033	NM_011633	TRCN0000040718
143				TRCN0000040719
144				TRCN0000040720
145				TRCN0000040721
146				TRCN0000040722
147	TRAF6	22034	NM_009424	TRCN0000040733
148				TRCN0000040734
149				TRCN0000040735
150				TRCN0000040736
151				TRCN0000040737
152	TRAF1	68015	NM_026508	TRCN0000112170
153				TRCN0000112171
154				TRCN0000112172
155				TRCN0000112173
156				TRCN0000112174
157				



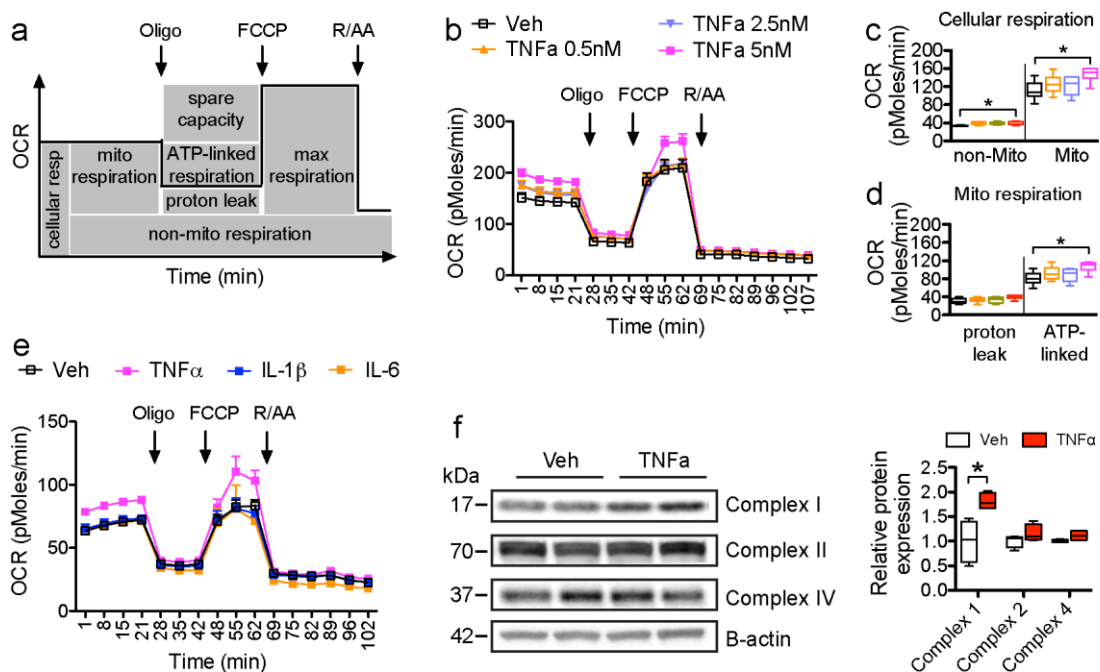
158

159 **Supplementary Figure 1.** The diurnal microglial activity patterns observed in chow-fed
 160 lean mice can be also observed in the MBH of rats on a chow diet, and fasting eliminates
 161 this diurnal pattern. (a-d) In chow-fed rats, although the difference in Iba1-ir cell
 162 number did not reach significance between ZT4 and ZT16 ($n=6$ for ZT4 and ZT16, $p=0.051$), the
 163 number of Iba1-ir cell processes in the MBH at ZT16 was significantly higher than at ZT4
 164 ($p=0.003$). (e-h) Illustration of the Iba1-ir cells in 24-h fasted lean or DIO mice. Cell
 165 number and processes per cell were quantified in a 0.2×0.2 -mm frame outlined by dashed
 166 lines in e, high magnification of the cells pointed at by dark arrows is presented at the left-
 167 upper corner of each picture. (i and j) Fasting for 24 h eliminated the interaction between
 168 time and body weight on Iba1-ir cell number and the number of processes in lean and DIO
 169 mice, there was an effect of body weight at ZT4 and ZT16 ($n=5$ for ZT4 and ZT16 of lean
 170 mice, $n=6$ for ZT4 and $n=5$ for ZT16 of DIO, for effect of bodyweight on Iba1-ir cell
 171 number, $F(1,17)=32.76$, $p<0.0001$; for effect of body weight on Iba1-ir cell processes,
 172 $F(1,17)=241.9$, $p<0.0001$), and there was an effect of time in DIO mice, $t_{10}=2.962$,
 173 $p<0.05$). (k) Fasting down-regulated, while refeeding stimulated, TNF α gene expression in
 174 the MBH of lean mice ($F(1,15)=4.377$, $p=0.032$). Scale bar: $160 \mu\text{m}$ in a, b, $200 \mu\text{m}$ in e-h.
 175 III: 3rd cerebral ventricle. * $P<0.05$, ** $P<0.01$, *** $P<0.001$. Data are presented as means \pm
 176 s.e.m. P values were analyzed by two-tailed Student's t test for unpaired comparisons in c,
 177 d, by two-way ANOVA followed by Bonferroni multiple comparisons in i, j; and by one-
 178 way ANOVA followed by post hoc t test in k.



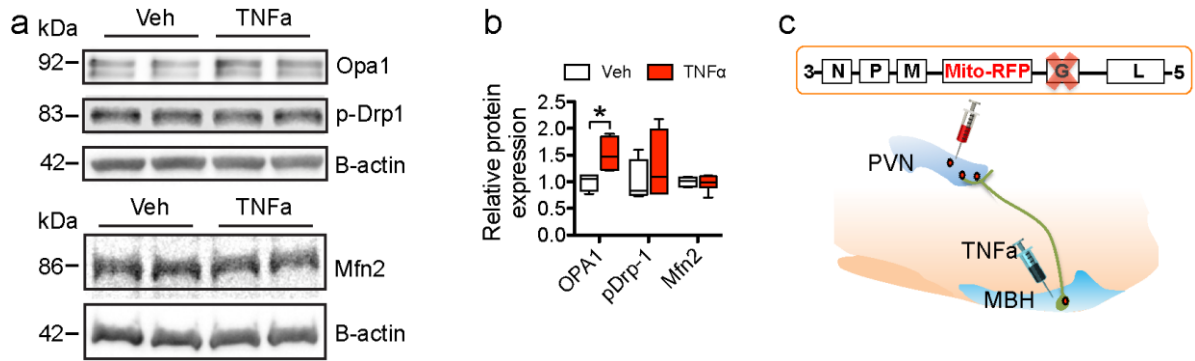
179

180 **Supplementary Figure 2.** Illustrations of the ultrastructure of microglial-neuronal soma
 181 very close contact in the hypothalamic arcuate nucleus (M: microglia, outlined in green, N:
 182 neuron, outlined in orange; *: nucleus of each cell). Arrows point to the contacting areas.
 183 Scale bar: 2 μ m in a and c, 1 μ m in b and d.



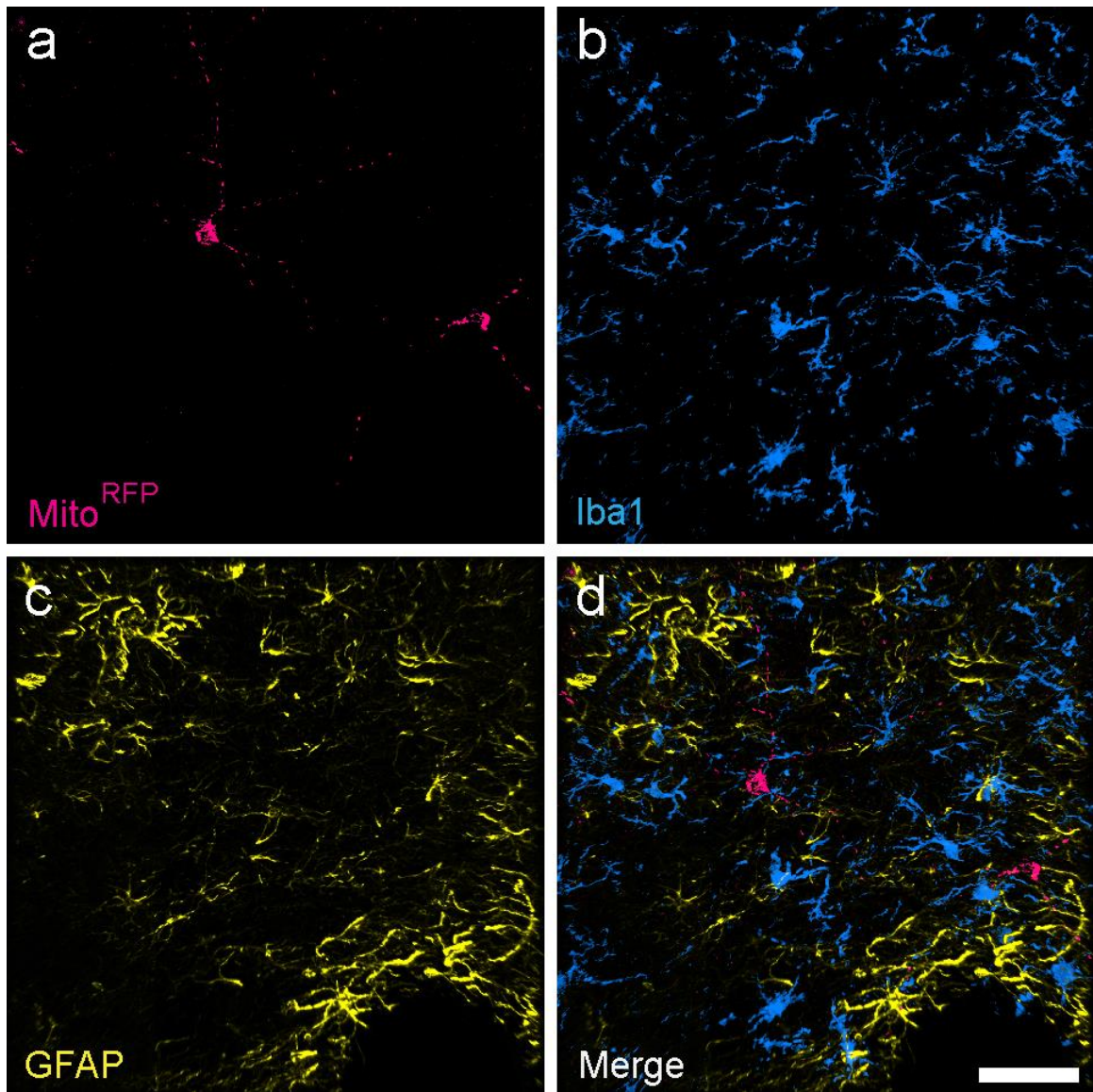
184

185 **Supplementary Figure 3.** TNF α stimulates hypothalamic neuronal mitochondrial activity.
 186 (a) Scheme depicting dissection of the oxygen-consuming processes of neurons. Cellular
 187 respiration was divided into mitochondrial and non-mitochondrial respiration using the
 188 ETC inhibitors rotenone (R) and antimycin A (AA). Mitochondrial respiration was further
 189 dissected into proton-leak and ATP-linked respiration using the ATP-synthase inhibitor
 190 oligomycin (Oligo). Maximal respiration was obtained after addition of an uncoupler
 191 (FCCP) and by subtracting the nonmitochondrial respiration rates. The portion of spare
 192 respiratory capacity was obtained by subtracting basal respiration from maximal
 193 respiration rates. Mitochondrial coupling efficiencies were calculated as the fraction of
 194 mitochondrial oxygen consumption that is sensitive to oligomycin, reflecting the fraction
 195 used to drive ATP synthesis. (b) Dose response of oxygen consuming rate (OCR)
 196 over time in primary hypothalamic neurons in response to different concentrations of TNF α . (c-
 197 d) Neurons treated by 5 nM TNF α had a significantly higher mitochondrial and ATP-
 198 linked oxygen consumption rate in comparison to those treated by vehicle, 0.5 nM or 2.5
 199 nM TNF α . In addition, neurons treated with 5 nM TNF α also had a significantly higher
 200 non-mitochondrial OCR. (e) OCR over time in primary hypothalamic neurons treated with
 201 TNF α , IL-1 β , IL-6, or vehicle. (f) Hypothalamic neurons treated with TNF α had
 202 significantly increased protein expression of complex-I, but not complex-II, or complex-IV
 203 (n=4 for each group, p=0.012 for complex-I). *P<0.05. Data are presented as means \pm
 204 s.e.m in b, and min to max in d. P values were analyzed by Student's *t* test. See also
 205 Supplementary Fig 10.



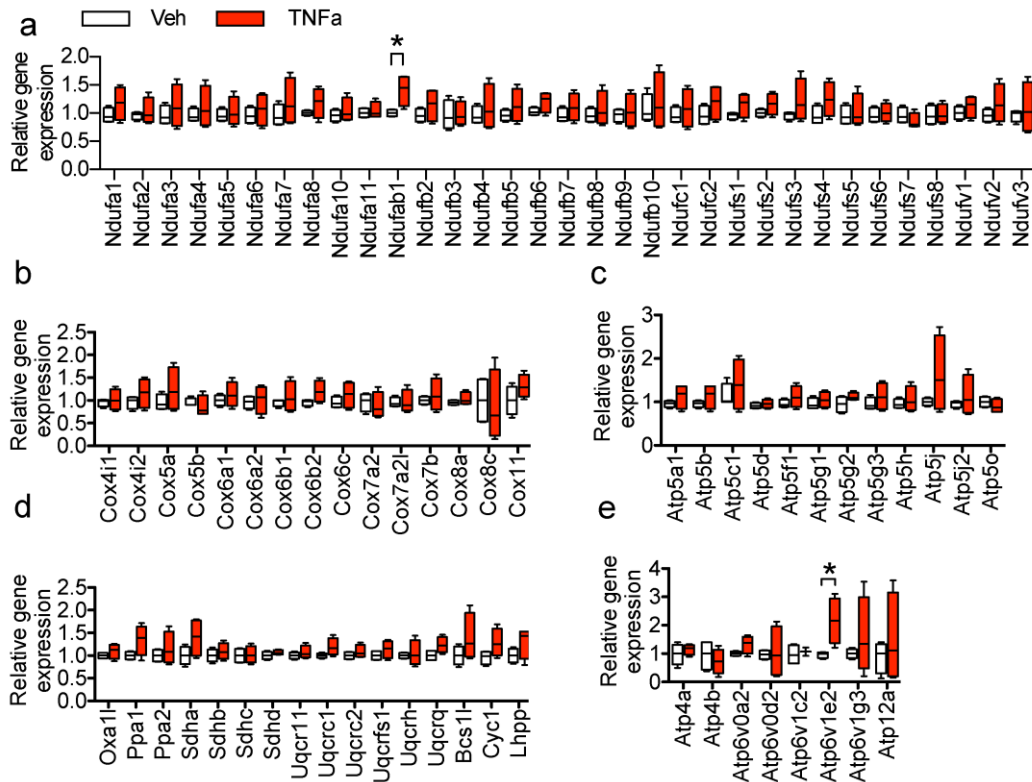
206

207 **Supplementary Figure 4.** TNF α stimulates hypothalamic neuronal mitochondrial fusion
 208 processes. Pseudotyped rabies virus (RABV Δ G) was produced to analyze mitochondrial
 209 fusion-fission processes in *in vivo*. (a and b) Hypothalamic neurons treated with TNF α had
 210 significantly increased protein expression of optic atrophy 1 (Opa1), but not of mito-fusion
 211 2 (Mfn2) or the phosphorylated dynamin-related protein 1 (p-Drp1) (n=4 for each group in
 212 Opa1 and p-Drp1 and n=6 for each group in Mfn2, p=0.034 for Opa1), see also
 213 Supplementary Fig 11. (c) The construction of RABV Δ G encoding for mitochondrially-
 214 targeted red fluorescence protein (Mito^{RFP}), and the schematic illustration of virus injection
 215 into the paraventricular nuclei (PVN) and the TNF α injection into the mediobasal
 216 hypothalamus (MBH). *P<0.05. Data are presented as min to max in b. P values was
 217 analyzed by Student's *t* test.
 218



219

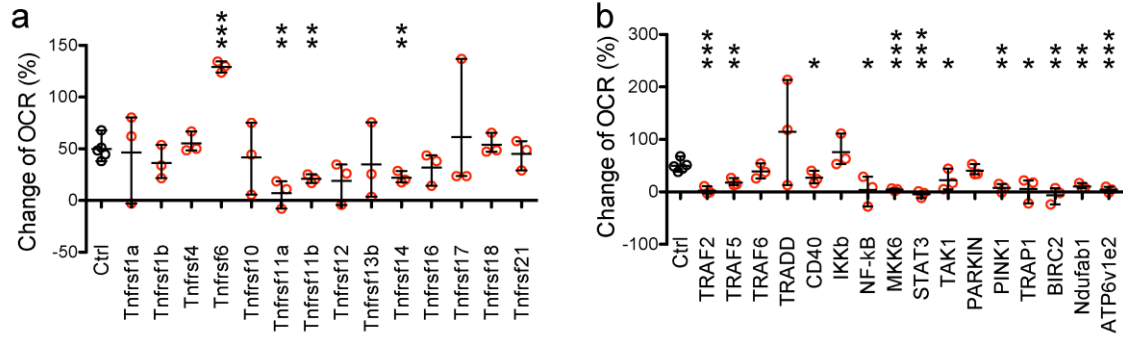
220 **Supplementary Figure 5.** Hypothalamic neurons infected by Mito^{RFP}-expressing
 221 RABVΔG did not stimulate immune responses from surrounding glial cells. (a)
 222 Hypothalamic neurons infected by Mito^{RFP}-expressing RABVΔG have Mito^{RFP}-labelled
 223 mitochondria. (b-d) No increase of iba1-ir microglia or GFAP-ir astrocytes occurred
 224 surrounding the PRV-infected neurons. Scale bar: 30 μm.
 225



226

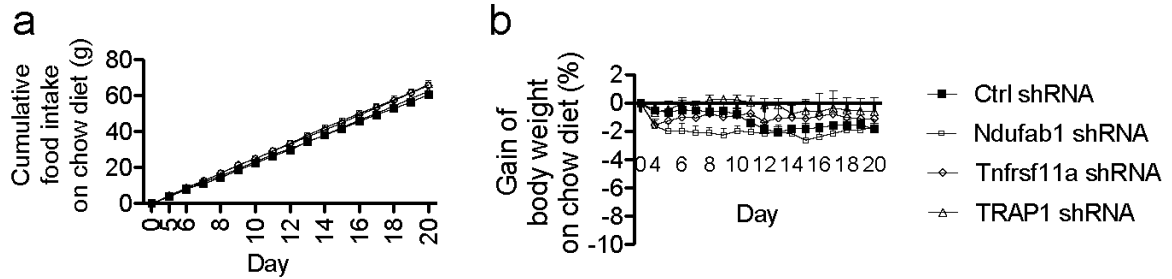
227 **Supplementary Figure 6.** Mitochondrial Energy Metabolism PCR Array in vehicle versus
 228 TNF α treatment in hypothalamic neurons. TNF α stimulated Atp6v1e2 (ATPase, H+
 229 transporting, lysosomal V1 subunit E2) and Ndufab1 (NADH dehydrogenase (ubiquinone)
 230 1, alpha/beta, subcomplex 1) gene expression (n=4 wells for vehicle and n=4 wells for
 231 TNF α , p=0.026 for Atp6v1e2, and p=0.031 for Ndufab1). NDUF: NADH dehydrogenase
 232 (ubiquinone), COX: Cytochrome c oxidase, ATP5: ATP synthase, Bcs1l: BCS1-like
 233 (yeast), Cyc1: Cytochrome c-1, Lhpp: Phospholysine phosphohistidine inorganic
 234 pyrophosphate phosphatase, Oxa11: Oxidase assembly 1-like, Ppa: Pyrophosphatase
 235 (inorganic), Sdh: Succinate dehydrogenase complex, Uqcr: Ubiquinol-cytochrome c
 236 reductase. *p<0.05. Data are presented as min to max. P values were analyzed by Two-
 237 tailed Student's t test for comparing vehicle versus TNF α .

238



239

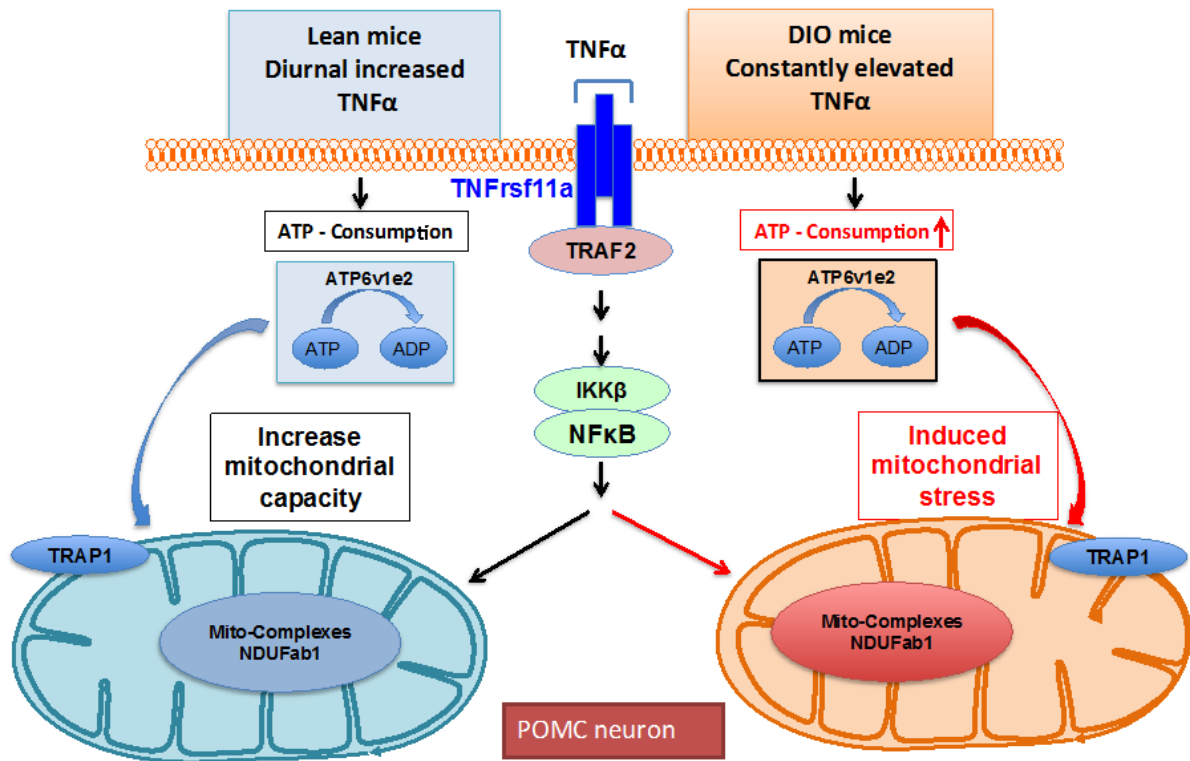
240 **Supplementary Figure 7.** Changes of cellular oxygen consuming rate (OCR) after
 241 knocking down each gene from the gene list of TNF receptors, the TNF receptor
 242 superfamily, and the TNF downstream-signalling pathway. (a) Changes of OCR with
 243 knocked down TNF receptors, and the TNF receptor superfamily ($F(1,36)=3.600$,
 244 $p=0.001$), knocked down Tnfrsf11a, 11b or 14 significantly attenuated the stimulatory
 245 effect of TNF α on OCR in comparison to Ctrl ($t_6=4.868$, $p=0.003$ for Tnfrsf11a, $t_6=4.219$,
 246 $p=0.006$ for Tnfrsf11b, $t_6=3.936$, $p=0.008$ for Tnfrsf14); knocking down Tnfrsf6 enhanced
 247 the stimulatory effect of TNF α on OCR ($p<0.001$). (b) Changes of OCR after knocking
 248 down the TNF downstream-signalling pathway ($F(1,36)=4.000$, $p=0.0003$); knocking
 249 down TNF receptor-associated factors 2 and 5 (TRAF2 and TRAF5, which mediate TNF
 250 effects on activation of MAPK8/JNK and NF- κ B) significantly attenuates or completely
 251 blocks the TNF-stimulatory effects on OCR ($t_6=6.487$, $p=0.0006$ for TRAF2, and $t_6=4.340$,
 252 $p=0.0005$ for TRAF5). Among the rest of the TNF-downstream signals, knocking down
 253 cluster of differentiation (CD40), NF- κ B, MAP kinase kinase 6 (MKK6), nuclear
 254 transcription factor signal transducer and activator of transcription 3 (STAT3, which can
 255 bind to mitochondrial DNA to regulate mitochondrial gene expression), the PTEN-induced
 256 putative kinase 1 (PINK1, mediating parkin protein-induced mitochondrial autophagy),
 257 TNF receptor-associated protein (TRAP1, a mitochondrial chaperone that regulates the
 258 metabolic switch between mitochondrial respiration and aerobic glycolysis), or apoptotic
 259 repression factor baculoviral inhibitors of apoptosis repeat-containing 1 (Birc1), can
 260 significantly attenuate or completely block the stimulatory effects of TNF on OCR
 261 ($t_6=6.487$, $p=0.034$ for CD40, $t_6=3.380$, $p=0.015$ for NF- κ B, $t_6=6.778$, $p=0.0005$ for
 262 MKK6, $t_6=7.511$, $p=0.0003$ for STAT3, $t_6=2.580$, $p=0.042$ for TAK1, $t_6=5.686$, $p=0.001$
 263 for PINK1, $t_6=3.619$, $p=0.011$ for TRAP1, $t_6=5.922$, $p=0.001$ for BIRC2). Furthermore,
 264 knocking down the selected mitochondrial targets, the mitochondrial respiratory chain
 265 complex-1 subunit - NADH dehydrogenase ubiquinone 1, alpha/beta subcomplex 1
 266 (Ndufab1), or the V-type proton ATPase subunit e2 (ATP6v1e2), completely blocked the
 267 TNF-stimulatory effects on OCR ($t_6=5.594$, $p=0.001$ for Ndufab1, $t_6=6.470$, $p=0.0006$ for
 268 ATP6v1e2). * $P<0.05$, ** $P<0.01$, *** $P<0.001$. Data are presented as means \pm s.e.m. P
 269 values were analyzed by One-way ANOVA followed by post hoc t test.
 270



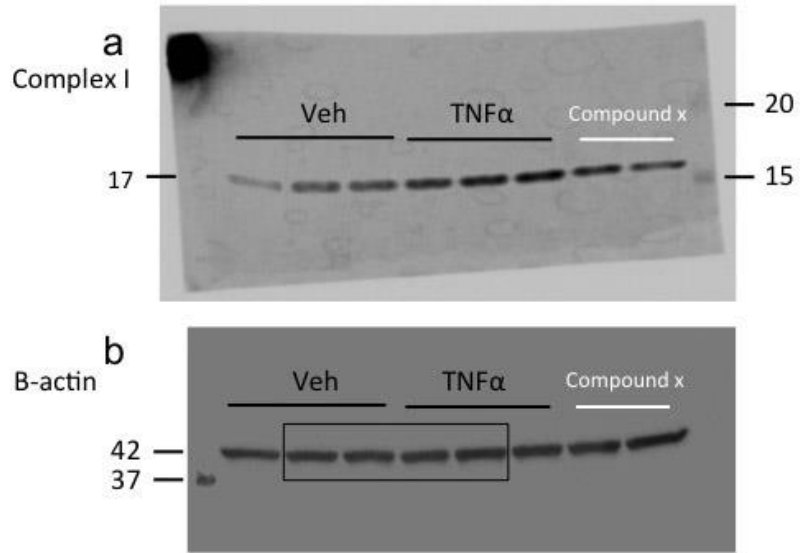
271

272 **Supplementary Figure 8.** Knocking down TNF α downstream signals by AAV-expressing
 273 Ndufab1 shRNA (n=5), Tnfrsf11a shRNA (n=4), or TRAP1 (n=4) in the MBH of chow-
 274 fed lean mice does not affect the food intake (a) or body weight gain (b), in comparison to
 275 mice that received AAV-expressing scrambled shRNA (F(1,15)=1.665, p=0.217 for food
 276 intake, and F(1,15)=0.574, p=0.641 for weight gain). Data are presented as means \pm s.e.m.
 277 P values were analyzed by One-way ANOVA followed by post hoc *t* test for comparing
 278 daily food intake or bodyweight gain between scrambled shRNA group and each of the
 279 three-targeted shRNA groups.

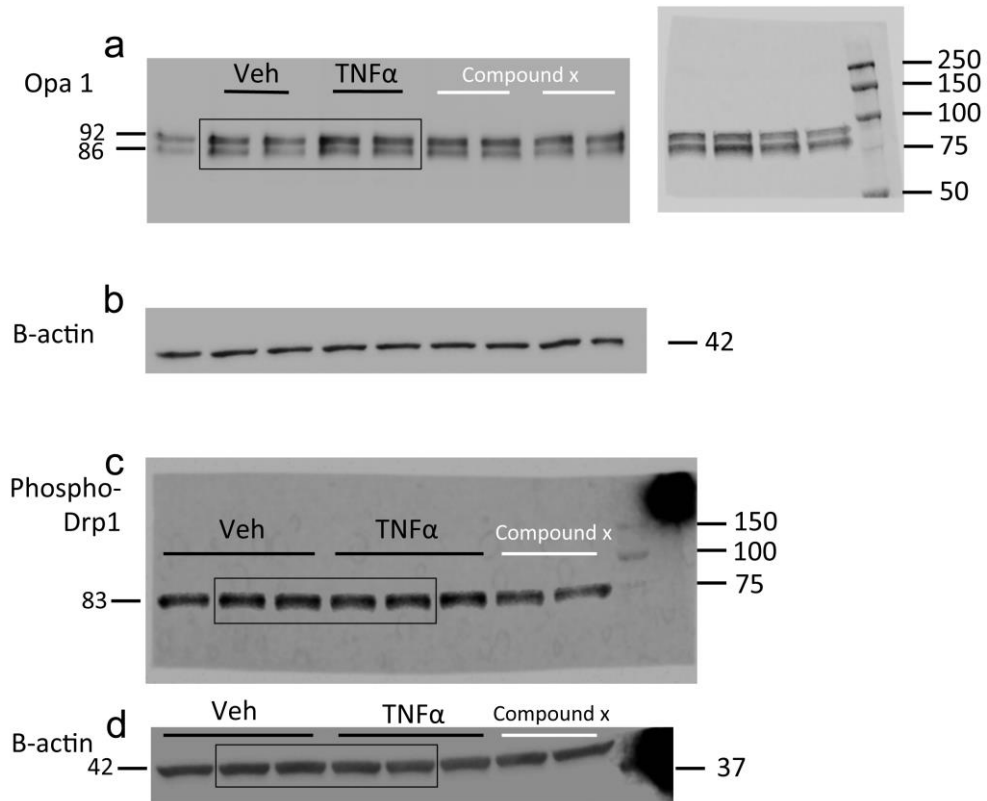
280



Supplementary Figure 9. In lean mice, TNF α engagement of TNFRsf11a activates NF- κ B signaling pathway and enhances complex-1 activity to promote mitochondrial ATP production, consequently matching ATP production with demands in neurons in the dark phase. In DIO mice, constantly elevated TNF α drives persistent mitochondrial activity and causes mitochondrial stress in POMC neurons.



288
289 **Supplementary Figure 10.** Uncropped blots of Complex I (a) and B-actin (b) of
290 supplementary figure 3f.



291
292
293
294
295

Supplementary Figure 11. Uncropped blots of Opa1 (a), p-Drp1 (c) and B-actin (d) of supplementary figure 4a. The image of the B-actin from Opa1 blot in b is not used in the figure. Instead, B-actin from p-Drp1 blot is presented).